TUM

TECHNISCHE UNIVERSITÄT MÜNCHEN
INSTITUT FÜR INFORMATIK

CampRecon
a software framework for linear inverse problems

Matthias Wieczorek, Jakob Vogel, Tobias Lasser

TUM-I1401

CampRecon — a software framework for linear inverse problems

Matthias Wieczorek, Jakob Vogel, and Tobias Lasser
Computer Aided Medical Procedures (CAMP), Technische Universität München, Germany
wieczore@cs.tum.edu

***Abstract*—This report describes a flexible, object-oriented software framework for modelling linear inverse problems, including solvers for analytic and least-squares solutions with optional regularization. Real-world linear problems can be composed at runtime, making the library suitable for a broad variety of applications. We demonstrate this flexibility with examples from X-ray Computed Tomography for linear attenuation and differential phase contrast.**

I. Introduction and Overview

THE reconstruction of physical quantities from measured signals is typically stated as an inverse problem. For the purpose of this work, we assume a linear measurement model, i.e. a linear relation between the physical quantities and the measured values. Application examples include different variants of tomographic reconstruction [1], image denoising [2][3], deconvolution and super-resolution[4].

Mathematically, we are interested in problems of the type

$$\mathcal{A}(x) = y, \quad \mathcal{A} \text{ linear operator} \tag{1}$$

where the linear relation $\mathcal{A}$ and the right-hand side y are known, and we seek to solve for x. For this work, we focus on large-scale problems where a discrete representation of $\mathcal{A}$ will exceed the memory of present-day computers by far. On top of that, the inverse problem is assumed to be ill-posed, therefore not directly (or only poorly) solvable in the presence of noise.

In the following, we will introduce the mathematical notations before describing the major components of our software framework. We will then demonstrate the application of the framework in a case-study using X-ray CT with attenuation contrast and differential phase contrast.

II. Mathematical Notations

Formalizing equation (1), we define a linear problem as follows:

Definition II.1 (Linear Problem). *Let X, Y denote two Hilbert spaces, and $\mathcal{A} \in \mathcal{L}(X, Y)$ a linear operator. Further, we assume $y \in \operatorname{im}(Y)$ to be known such that $\exists x \in X$:*

$$\mathcal{A}(x) = y. \tag{2}$$

The inverse problem to (2) *consists of finding a $x \in X$, such that $\mathcal{A}(x) = y$ holds.*

Note that if $\mathcal{A}$ is invertible, the solution to this inverse problem is uniquely given by $x = \mathcal{A}^{-1}(y)$.

The linear problem is completely defined by $y \in Y$ and $\mathcal{A} \in \mathcal{L}(X, Y)$. Furthermore, X, Y may be function spaces (such as $\mathcal{L}^p$), for example when modeling an image or signal as a function $f : \Omega \to \mathbb{R}$, where Ω denotes some coordinate set.

Informally, y contains measurements or observations, and $\mathcal{A}$ is a linear model of how the (unknown) signal x causes the observations. In practice, the measurements will be corrupted by noise, denoted by $\xi \in Y$, and instead of y, we only know $y + \xi$.

To represent the linear problem on computers, we use the following conventions:

Definition II.2 (Discretization). *Let $f : X \to Y$ denote a function between two Hilbert spaces X, Y, and $\{b_i\}_{i \in I}$ a finite set of basis functions $b_i : X \to Y$ such that f can be written as their linear combination:*

$$f = \sum_{i \in I} x_i b_i \tag{3}$$

*The coefficient vector $x = \{x_i\}_{i \in I}$ is called the **discretization** of f.*

Please note that in real-world scenarios discretization most likely will introduce discretization errors. For simplicity, we will neglect these errors noting that in practice equality will be replaced by approximated equality.

Lemma II.3. *Let W, X, Y, Z be Hilbert spaces with functions $f \in X^Y$ and $g \in W^Z$, and an operator $\mathcal{A} \in \mathcal{L}(X^Y, W^Z)$ such that $\mathcal{A}(f) = g$.*

Further, let x denote a discretization of f with respect to $\{b_i\}_{i\in I}$, $b_i \in X^Y$, and y a discretization of g with respect to $\{c_j\}_{j\in J}$, $c_j \in W^Z$. Then, $\mathcal{A}$ can be approximated by a finite-dimensional matrix $\mathbf{A}$ as follows:

$$\sum_{j\in J} y_j c_j = g = \mathcal{A}(f)$$
$$= \sum_{i\in I} x_i \underbrace{\mathcal{A}(b_i)}_{\in W^Z}$$
$$= \sum_{i\in I} x_i \sum_{j\in J} a_{i,j} c_j$$
$$= \sum_{j\in J} \left(\sum_{i\in I} a_{i,j} x_i \right) c_j$$

This leads to $y = \mathbf{A}x$, where the columns $a_{\cdot,j}$ of matrix $\mathbf{A}$ equal the discretization of $\mathcal{A}(b_i)$ with respect to $\{c_j\}_{j\in J}$.

In words, the matrix $\mathbf{A}$ approximates the linear operator $\mathcal{A}$ using discretization within its range as well as its domain.

Again please note, that in practice these discretizations most probably cause errors. In order to cope with that, we instead aim at minimizing $\min_x \|\mathbf{A}x - y\|$ using some norm, instead of solving the equation directly.

As an illustration of this mathematical formulation, we show two concrete examples in the setting of two-dimensional X-ray CT, one for attenuation contrast, one for differential phase contrast. Other tomographic imaging modalities such as PET, SPECT or optical tomography, can be represented in a similar manner.

A. X-ray attenuation CT

The goal of X-ray attenuation CT is the reconstruction of the linear attenuation coefficient $f : \mathbb{R}^2 \to \mathbb{R}$ of an unknown object from X-ray projection data. The acquisition process is modeled by the *Radon transform*

$$\mathcal{R}f(\theta, s) := \int_{L(\theta,s)} f(x)\,\mathrm{d}x \qquad (4)$$

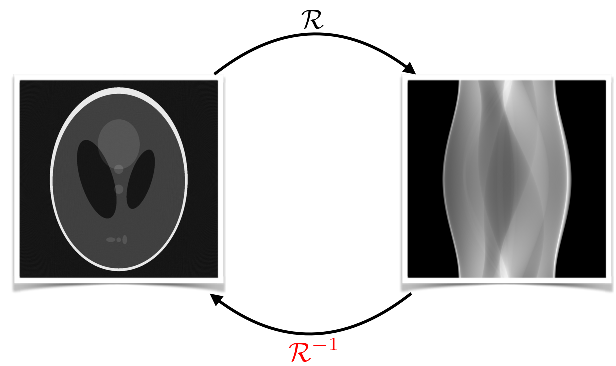

Fig. 1: Computed tomography – a linear problem using the Radon transform $\mathcal{R}$.

where $L(\theta, s) = \{x \in \mathbb{R}^2 : \; x_1 \cos\theta + x_2 \sin\theta = s\}$ denotes the line with normal $(\cos\theta, \sin\theta)^T$ and (signed) distance $s \in \mathbb{R}$ from the origin.

Using lemma II.3, the discretized version (also called *series expansion*) reads as follows: Given a finite set of measurements $(y_m)_{m=1}^M$ (assumed to form a discretization of $\mathcal{R}f$), the unknown function f is expanded with respect to a given basis $(\psi_n)_{n=1}^N$ via $f = \sum_{n=1}^N x_n \psi_n$. Then, the discretization $(x_n)_{n=1}^N$ is determined from the measurements,

$$y_m = \mathcal{R}f(\theta_m, s_m) = \sum_{n=1}^{N} x_n \mathcal{R}\psi_n(\theta_m, s_m) \qquad (5)$$

This yields the linear problem $\mathbf{R}x = y$, see Fig. 1.

B. Differential phase contrast CT

X-ray differential phase contrast imaging (DPCI) can be modeled similar to X-ray attenuation imaging [5], [6], [7], but measuring a differential signal of the phase shift instead of attenuation values. An appropriate mathematical model is:

$$\mathcal{P}f(\theta, s) := \frac{\partial}{\partial s} \int_{L(\theta,s)} f(x)\,\mathrm{d}x \qquad (6)$$

Again, this can be turned into a linear problem using series expansion, and we write $\mathbf{P}x = y$. Due to the structure of $\mathbf{P}$ we can decompose this operator into a differential operator and the Radon operator: $\mathbf{P} = D * \mathbf{R}$.

III. Software Framework

For solving linear inverse problems, we designed an object-oriented software framework, consisting of

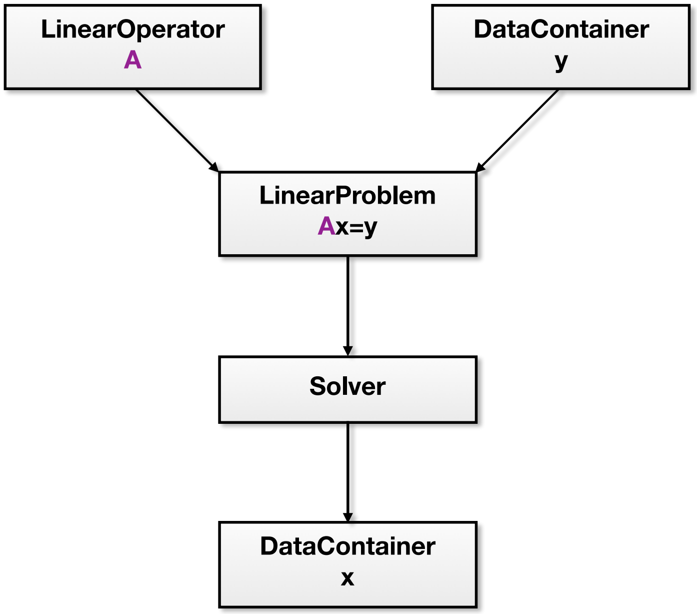

Fig. 2: Flow chart – Solve linear problem

the components depicted in Fig. 2. In more detail, the components are:

- A **DataContainer** handling discrete representations of signals (functions) as serialized data. Meta data describing the discretization and the nature of the serialized data is held within a **DataDescriptor**. Furthermore, a dictionary transform may be attached to represent data in different bases / frames [8], for instance the Fourier basis or Wavelet, Curvelet frames.
- A hierarchy of **LinearOperator** classes providing a generalized representation of the corresponding mathematical counterpart. In particular, we offer means to concatenate such operators using text expressions and operator composites.
- Class **LinearProblem** combines such a (potentially composite) linear operator $\mathcal{A}$ with measurements y.
- A set of **Solver** classes to implement algorithms to compute or approximate solutions for such linear problems. We provide analytical as well as iterative solvers, with or without regularization (in particular ℓ_1-based penalties).

As the variety of problems we are able to tackle depends on the implementation of the according LinearOperator, we will focus on this part of our framework. The **LinearOperator** class provides an abstract definition of elements of $\mathcal{L}(X, Y)$ as described in lemma II.3. While we support explicit matrix representation, our main objective are operators for which the explicit formulation exceeds system memory. For this purpose we define linear operators abstractly, requiring implementations to provide two methods:

- *apply(x)*, computing $\mathcal{A}(x)$
- *applyAdjoint(x)*, computing $\mathcal{A}^*(x)$ ($\mathcal{A}^\top x$ in case of a real-valued operator)

This leaves vital optimizations such as closed form index calculations (for differential operators) or GPU ray-casting (for Radon operators) to specialized implementations.

At the time of writing, we support a number of such concretizations:

A. Basis and frame transformations

Apart from the pixel basis, representing data in a different frame [8] may be preferable to exploit properties such as sparsity of Wavelet coefficients, or compact support in Fourier space. We currently support two transforms, Fast Fourier Transform (FFT) and Curvelet transform [9], [10]. Further transforms such as Wavelets[11], spherically symmetric basis functions ('blobs') [12], etc. can be added as needed.

B. Fourier convolution

Following the convolution theorem for two integrable functions f, g, we provide a discretized convolution operator for a given convolution filter g using the FFT operator as follows:

$$\mathcal{C}_g(f) = g * f = \mathcal{F}^{-1}\{\mathcal{F}\{g\} \cdot \mathcal{F}\{f\}\} \tag{7}$$

C. Radon operator

For the purpose of X-ray computed tomography, we support several implementations of the Radon operator as described previously. These include CPU-based and highly optimized GPU projectors for the pixel basis, but also a closed-form projector for the Curvelet frame [13].

For other imaging modalities, suitable operators can be implemented in a similar manner.

D. *Differential operator*

As approximation to the differential operator, we provide finite differences (forward, central and backward) for the pixel basis.

E. *LinearOperatorComposite*

Based on linear operator arithmetic we implemented the **LinearOperatorComposite** class to support recursive concatenation of linear operators. In order to simplify its use, the concatenation is constructed using a textual representation, supporting the binary operators `+`, `-`, `*`, and the unary operator `^T`. Note that these operators are evaluated dynamically at run-time.

Using this modular principle, we enable formulation of a broad variety of linear inverse problems.

IV. Case-Studies

Returning to our case-study of X-ray computed tomography, we use the Shepp-Logan phantom [14] to generate virtual measurements for both attenuation and phase-contrast, by applying the respective forward models (4) and (6). As examples, we will study three linear solvers – one analytic and two iterative approaches – that are easily implemented with just a few statements using our framework.

To reconstruct other imaging modalities, one simply needs to provide an implementation of an appropriate forward model in form of a linear operator.

A. *Filtered Back-Projection*

Filtered Back-Projection (FBP) constitutes an analytic solver to the Radon-problem (4). Let $\mathcal{R} \in \mathcal{L}(\mathcal{L}^1, \mathcal{L}^1)$ denote the Radon operator, and $\mathcal{C} \in \mathcal{L}(\mathcal{L}^1, \mathcal{L}^1)$ the convolution operator as described in section III-B. Then,

$$x = (\mathcal{R}^\top \circ \mathcal{C})(y) \tag{8}$$

is the inversion of the Radon problem [1].

In our framework, this solver can be expressed using the **LinearOperatorComposite** as illustrated in Fig. 3, showing the logical flow chart as well as a reconstruction result for the Shepp-Logan phantom.

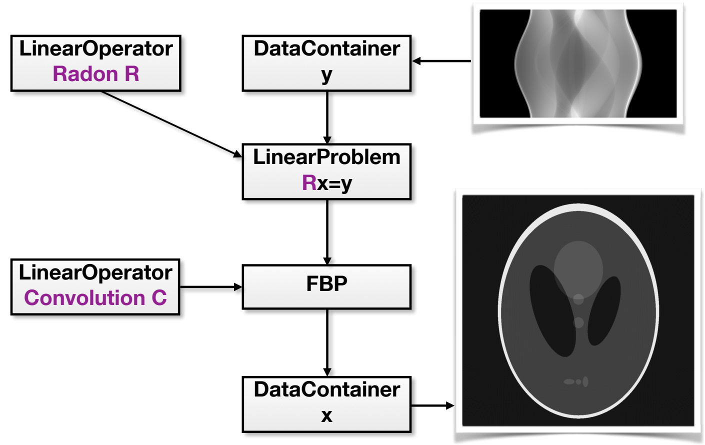

Fig. 3: Flow chart for FBP reconstruction

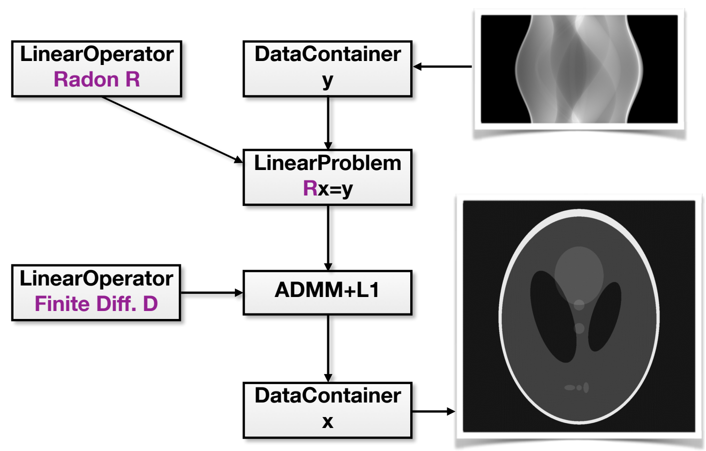

Fig. 4: Flow chart for CT reconstruction using TV-penalty

B. *Alternating Direction Method of Multipliers for ℓ_1-regularized linear regression*

Furthermore, we support the Alternating Direction Method of Multipliers (ADMM) for the special case of ℓ_1-regularized linear regression as described in [15]. Assuming a linear operator $\mathcal{T} \in \mathcal{L}(X, Y)$ such that $\mathcal{T}(x)$ is sparse, solving the ℓ_1-regularized problem

$$\arg\min_x \frac{1}{2} \|\mathcal{R}(x) - y\|_2^2 + \lambda \|\mathcal{T}(x)\|_1 \tag{9}$$

yields a suitable reconstruction [16]. Examples for such $\mathcal{T}$ are the differential operator (leading to total variation regularization) or wavelet/frame transforms (providing special sparsity properties). Fig. 4 reproduces the flow chart and the result of a TV-regularized ADMM reconstruction for CT.

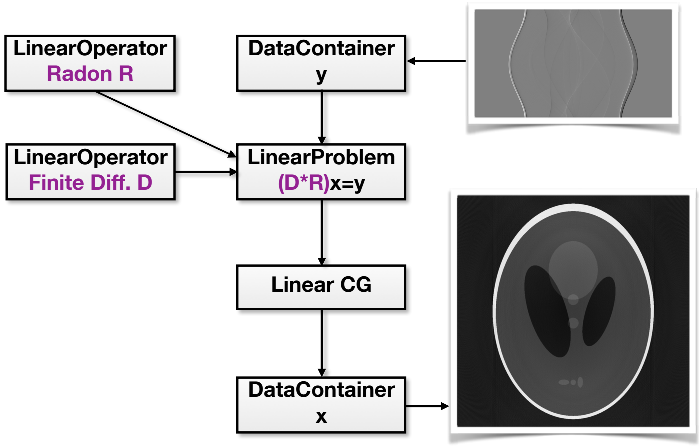

Fig. 5: Flow chart for DPCI CT

C. Linear Conjugate Gradient

The Conjugate Gradient (CG) method [17] is a well-known iterative solver for linear inverse problems. In its standard configuration, the operator is required to be symmetric and positive definite. Our framework keeps track of whether this is the case for a given setup, and if not, falls back to solving the least squares problem via the normal equation. In case of the DPCI CT, we solve

$$\arg\min_{x} \frac{1}{2} \|\mathcal{P}(x) - y\|_2^2 \tag{10}$$

via the normal normal equation

$$\mathcal{P}^\top \mathcal{P}(x) = \mathcal{P}^\top y. \tag{11}$$

Using the **LinearOperatorComposite**, we model the linear operator for DPCI using a differential and a radon operator and solve it using linear CG, as shown in Fig. 5.

V. Conclusion

In this work we present a flexible, object-oriented software framework mapping the properties of linear operators and linear problems into software, and providing solvers to compute solutions to the resulting inverse problems. Focusing on ill-posed, large-scale inverse problems and composition of operators, this framework is widely applicable and can be extended to a broad variety of applications, such as the various tomographic imaging modalities. As an example, we presented applications to X-ray CT imaging of attenuation contrast and phase contrast.

References

[1] F. Natterer, *The Mathematics of Computerized Tomography*, ser. Classics in Applied Mathematics. Society for Industrial and Applied Mathematics, 2001.

[2] L. I. Rudin, S. Osher, and E. Fatemi, “Nonlinear total variation based noise removal algorithms,” *Physica D: Nonlinear Phenomena*, vol. 60, no. 1, pp. 259–268, 1992.

[3] D. Strong and T. Chan, “Edge-preserving and scale-dependent properties of total variation regularization,” *Inverse problems*, vol. 19, no. 6, p. S165, 2003.

[4] M. Elad and A. Feuer, “Restoration of a single superresolution image from several blurred, noisy, and undersampled measured images,” *Image Processing, IEEE Transactions on*, vol. 6, no. 12, pp. 1646–1658, 1997.

[5] T. Köhler, B. Brendel, and E. Roessl, “Iterative reconstruction for differential phase contrast imaging using spherically symmetric basis functions,” *Medical Physics*, vol. 38, no. 8, p. 4542, 2011.

[6] M. Nilchian, C. e. d. Vonesch, P. Modregger, M. Stampanoni, and M. Unser, “Fast iterative reconstruction of differential phase contrast X-ray tomograms,” *Opt. Express*, vol. 21, no. 5, pp. 5511–5528, Mar. 2013.

[7] M. Wieczorek, J. Frikel, J. Vogel, F. Pfeiffer, L. Demaret, and T. Lasser, “Curvelet sparse regularization for differential phase-contrast X-ray imaging,” in *Proc. Int’l Meeting on Fully Three-Dimensional Image Reconstruction in Radiology and Nuclear Medicine (Fully3D)*, 2013.

[8] O. Christensen, *An Introduction to Frames and Riesz Bases*, ser. Applied and Numerical Harmonic Analysis. Birkhäuser Boston, 2002.

[9] E. Candes and D. Donoho, “Continuous Curvelet Transform: I. Resolution of the wavefront set,” *Applied and Computational Harmonic Analysis*, vol. 19, no. 2, pp. 162–197, 2005.

[10] ——, “Continuous Curvelet Transform: II. Discretization and Frames,” *Applied and Computational Harmonic Analysis*, vol. 19, no. 2, pp. 198–222, 2005.

[11] M. Unser and T. Blu, “Wavelet theory demystified,” *Signal Processing, IEEE Transactions on*, vol. 51, no. 2, pp. 470–483, 2003.

[12] R. M. Lewitt, “Multidimensional digital image representations using generalized Kaiser-Bessel window functions,” *Journal of the Optical Society of America A*, vol. 7, no. 10, p. 1834, 1990.

[13] J. Frikel, “Sparse regularization in limited angle tomography,” *Applied and Computational Harmonic Analysis*, vol. 34, pp. 117–141, 2013.

[14] L. A. Shepp and B. F. Logan, “The Fourier reconstruction of a head section,” *Nuclear Science, IEEE Transactions on*, vol. 21, no. 3, pp. 21–43, 1974.

[15] S. Boyd, “Distributed Optimization and Statistical Learning via the Alternating Direction Method of Multipliers,” *Foundations and Trends® in Machine Learning*, vol. 3, no. 1, pp. 1–122, 2011.

[16] I. Daubechies, M. Defrise, and C. De Mol, “An iterative thresholding algorithm for linear inverse problems with a sparsity constraint,” *Communications on pure and applied mathematics*, vol. 57, no. 11, pp. 1413–1457, 2004.

[17] J. R. Shewchuk, “An Introduction to the Conjugate Gradient Method Without the Agonizing Pain,” *An Introduction to the Conjugate Gradient Method Without the Agonizing Pain*, Mar. 1994.